

pubs.acs.org/JPCL Letter

# A Crossed Molecular Beams and Computational Study of the Formation of the Astronomically Elusive Thiosilaformyl Radical (HSiS, X<sup>2</sup>A')

Shane J. Goettl, Zhenghai Yang, Srinivas Doddipatla, Chao He, Márcio O. Alves, Breno R. L. Galvão,\* and Ralf I. Kaiser\*



Cite This: J. Phys. Chem. Lett. 2021, 12, 5979-5986



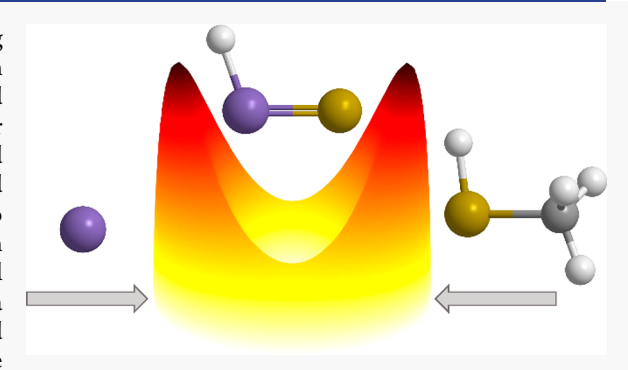
**ACCESS** 

III Metrics & More

Article Recommendations

Supporting Information

**ABSTRACT:** The formation pathways to silicon- and sulfur-containing molecules are crucial to the understanding of silicon-sulfur chemistry in interstellar and circumstellar environments. While multiple silicon- and sulfur-containing species have been observed in deep space, their fundamental formation mechanisms are largely unknown. The crossed molecular beams technique combined with electronic structure and Rice-Ramsperger-Kassel-Marcus (RRKM) calculations was utilized to study the bimolecular reaction of atomic silicon (Si( $^3P_i$ )) with thiomethanol (CH $_3$ SH, X $^1$ A $^\prime$ ) leading to the thiosilaformyl radical (HSiS, X $^2$ A $^\prime$ ) via an exclusive methyl radical (CH $_3$ , X $^2$ A $^\prime$ ) loss via indirect scattering dynamics which involves barrierless addition and hydrogen migration in an overall exoergic reaction, indicating the



possibility that HSiS can form in cold molecular clouds. The astronomically elusive thiosilaformyl radical may act as a tracer of an exotic silicon—sulfur chemistry to be deciphered toward, for example, the star-forming region SgrB2, thus leading to a better understanding of the formation of silicon—sulfur bonds in deep space.

he investigation of the formation and reactivity of sulfurbearing molecules in extraterrestrial environments represents an important instrument to understand the history and chemical evolution of star-forming regions, cold molecular clouds, and circumstellar envelopes of carbon stars. 1-3 Compared to the cosmic carbon versus sulfur ratio of 15:1, sulfur is severely depleted in carbon-containing molecules. Thiomethanol (methylmercaptan, CH<sub>3</sub>SH), the isovalent counterpart of methanol (CH<sub>3</sub>OH), represents one of 20 sulfur-carbon-bearing molecules detected in the interstellar medium (ISM) (Figure 1). Identified for the first time by Linke et al. in the star-forming region SgrB2<sup>4</sup> through its rotational spectrum<sup>5</sup> and confirmed by Turner,<sup>6</sup> Belloche et al.,<sup>7</sup> and Müller et al.,<sup>8</sup> the thiomethanol molecule has emerged as a potential molecular building block leading to sulfurcontaining amino acids like cysteine (HSCH2CH(COOH)-NH<sub>2</sub>) on low-temperature (10 K) ice-coated interstellar grains. On the basis of the detection of thiomethanol toward the solar type protostar IRAS 16293-2422<sup>10</sup> and the HH 212 protostellar disk,<sup>11</sup> Majumdar et al. proposed a formation of thiomethanol on low-temperature icy grains followed by sublimation and/or reactive desorption<sup>12</sup> into the gas phase. Lamberts's computational model<sup>13</sup> suggested that thiomethanol could be formed on grains from carbon monosulfide (CS) by stepwise hydrogenation via cis/trans-thiohydroxycarbene intermediates (HCSH) involving an analogous reaction

sequence from carbon monoxide (CO) to methanol (CH<sub>3</sub>OH). However, once released from the grains into the gas phase, the chemistry and reactivity of thiomethanol is not well-understood. Heavs et al. proposed that thiomethanol could be photodissociated and photoionized by the ultraviolet interstellar radiation field forming, e.g., CH<sub>3</sub>S<sup>+</sup>, CH<sub>2</sub>SH<sup>+</sup>, H<sub>2</sub>SCS<sup>+</sup>, and HCS<sup>+</sup>. Ion flow studies revealed that thiomethanol could be rapidly protonated upon reaction with the hydronium ion (H<sub>3</sub>O<sup>+</sup>). Nevertheless, bimolecular reactions of thiomethanol in the gas phase involving two neutral species and their role in the formation of (hitherto astronomically unobserved) sulfur-bearing species have not been explored to date in laboratory experiments.

Crossed molecular beam experiments represent an ideal approach to untangle the outcome of elementary gas-phase reactions leading to sulfur-bearing molecules and their radicals of astrochemical relevance. <sup>17–19</sup> Merging molecular beams and electronic structure calculations, Kaiser et al. <sup>20</sup> and Ochsenfeld

Received: May 29, 2021 Accepted: June 18, 2021



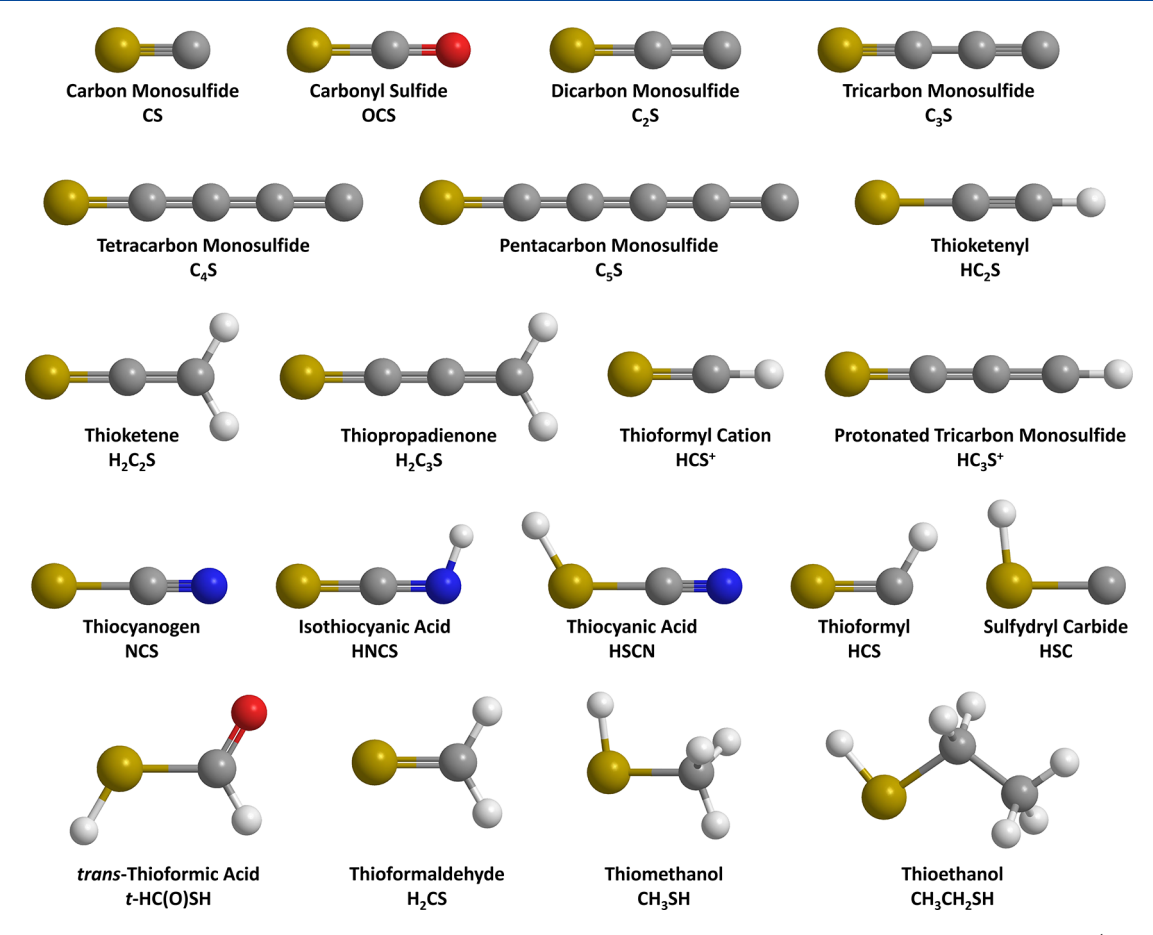


Figure 1. Sulfur—carbon-bearing molecules as detected in the interstellar medium. Atoms are color-coded as follows: sulfur (yellow); carbon (gray); oxygen (red); nitrogen (blue); hydrogen (white).

et al.<sup>21</sup> revealed that the reaction of ground-state carbon atoms  $(C(^{3}P_{i}))$  with hydrogen sulfide  $(H_{2}S)$  leads to the formation of the thioformyl radical (HCS, X<sup>2</sup>A") along with atomic hydrogen; reaction rates close to gas kinetics limits of a few 10<sup>-10</sup> cm<sup>3</sup> s<sup>-1</sup> were derived.<sup>22</sup> The thioketenyl radical (HCCS,  $X^2\Pi$ ) was assigned as the product of the bimolecular gas-phase reaction of dicarbon  $(C_2, X^1\Sigma_g^+)$  with hydrogen sulfide  $(H_2S)$ . A recent chemical dynamics study of the rapid methylidyne (CH)-hydrogen sulfide (H<sub>2</sub>S) reaction revealed the formation of thioformaldehyde (H<sub>2</sub>CS) as well as thiohydroxycarbene (HCSH) under the elimination of atomic hydrogen, <sup>23</sup> thus demonstrating the unique power of the crossed molecular beam approach to unravel molecular mass growth processes by coupling interstellar carbon with sulfur chemistry. Here, we provide new knowledge on elementary reactions of sulfurbearing molecules and unravel the chemical dynamics of the reaction of ground-state silicon atoms (Si(3P<sub>i</sub>)) with thiomethanol (CH<sub>3</sub>SH) under single-collision conditions exploiting molecular beams. Coupling interstellar silicon with sulfur chemistry reveals the formation of at least the astronomically hitherto undetected thiosilaformyl (HSiS, X<sup>2</sup>A') isomer through the atomic silicon (Si) versus methyl (CH<sub>3</sub>) exchange pathway. In deep space, these radicals might be photodissociated by the ultraviolet field, eventually forming interstellar and circumstellar silicon monosulfide (SiS), 24-27 molecular building block suggested to initiate a chain of reactions that lead ultimately to sulfide dust grains.<sup>28–30</sup>

The crossed molecular beam experiments probed the atomic (H) and molecular hydrogen  $(H_2)$  loss pathways (reactions 1)

and 2) as well as the methyl  $(CH_3)$  and methane  $(CH_4)$  elimination channels (reactions 3 and 4):

$$CH_3SH + Si(^3P_j) \rightarrow SiCH_3S + H$$
 (1)

$$CH_3SH + Si(^3P_j) \rightarrow SiCH_2S + H_2$$
 (2)

$$CH_3SH + Si(^3P_j) \rightarrow HSiS + CH_3$$
 (3a)

$$CH_3SH + Si(^3P_j) \rightarrow HSSi + CH_3$$
 (3b)

$$CH_3SH + Si(^3P_j) \rightarrow SiS + CH_4$$
 (4)

Accounting for the natural isotopic abundances of sulfur (32S, 94.9%; <sup>33</sup>S, 0.8%; <sup>34</sup>S, 4.3%), silicon (<sup>28</sup>Si, 92.2%; <sup>29</sup>Si, 4.7%; <sup>30</sup>Si, 3.1%), and carbon (<sup>12</sup>C, 98.9%; <sup>13</sup>C, 1.1%), the reactive scattering signal was searched for at mass-to-charge ratios of m/z = 75 and 74 for the atomic and molecular hydrogen loss channels and at 61 and 60 for the methyl and methane loss channels, respectively. Despite scanning at the center-of-mass angle of 54° for 10 h, no definite signal for channels 1 or 2 was observable. However, signal was observable for the methyl loss channel (reaction (3)) as evidenced from ion counts recorded at m/z = 61 (HSiS<sup>+</sup>) and 60 (SiS<sup>+</sup>) (Figure S1). The TOF spectra at m/z = 61 and 60 are superimposable, i.e., they overlap after scaling, suggesting that only a single reaction channel is open in this elementary reaction, and the signal at m/z = 60 originates from dissociative electron impact ionization of the neutral reaction product at 61 amu. The

TOF spectra are very broad and extend over  $500 \mu s$  (Figure 2). The corresponding laboratory angular distribution, which is

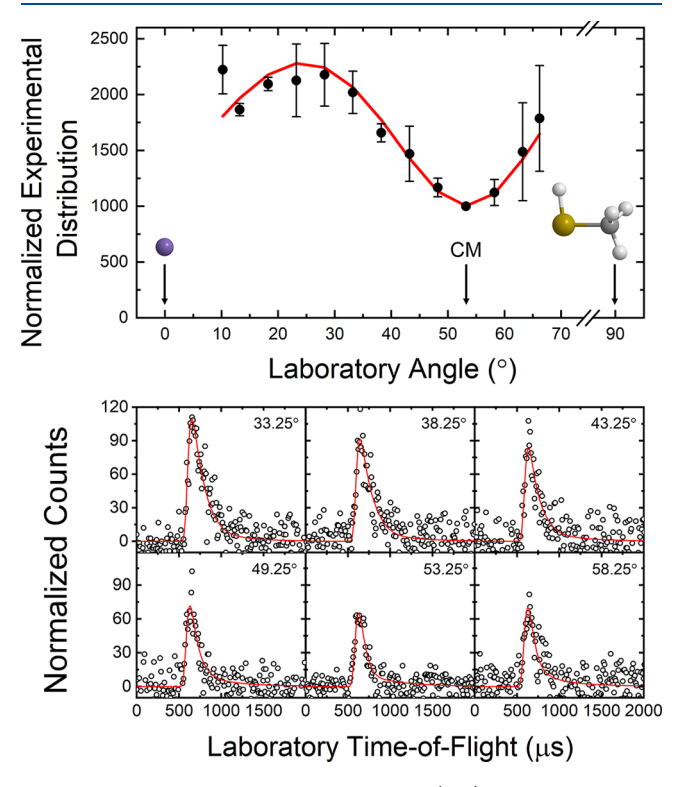


**Figure 2.** Laboratory angular distribution (top) and TOF spectra (bottom) for the reaction of atomic silicon  $(Si(^3P_j))$  with thiomethanol (CH<sub>3</sub>SH) recorded at m/z=61. The directions of the silicon and thiomethanol beams are  $0^\circ$  and  $90^\circ$ , respectively. The black circles denote the experimental data, with the red lines given as the best-fits obtained from the CM functions shown in Figure 3.

spread over the accessible laboratory angular range from  $10^{\circ}$  to  $67^{\circ}$  in the scattering plane, reveals a dip close to the center-of-

mass angle. This finding suggests indirect scattering dynamics through involvement of SiCH<sub>4</sub>S collision complex(es). An inspection of the corresponding Newton diagrams for the methyl and methane loss channels (reactions 3 and 4), respectively, reveals interesting findings (Figure S2). These diagrams correspond to the most probable velocities of the atomic silicon and thiomethanol reactants; the two-dimensional projection of the recoil spheres ("Newton circles") indicate the maximum velocities of the recoil vectors for channels 3 and 4 accounting for conservation of energy and momentum. Considering the predicted angular range of the H<sup>28</sup>Si<sup>32</sup>S/H<sup>32</sup>S<sup>28</sup>Si and <sup>28</sup>Si<sup>32</sup>S products, the Newton circles for the methyl and methane loss channels are distinct with the angular range of signal collected at m/z = 61 revealing close resemblance to the theoretically predicted distribution of the methyl group loss channel 3. The predicted angular range of the methane loss pathway (reaction 4) is significantly larger than the Newton circle of the methyl loss and could not account for the reactive scattering signal. Therefore, our laboratory data along with the Newton diagrams suggest the existence of the atomic silicon versus methyl group loss channel (reaction 3) and the absence of atomic and molecular hydrogen along with methane elimination pathways.

To offer quantitative evidence on the existence of the methyl loss channel (reaction 3) in the reaction of ground-state atomic silicon with thiomethanol and to reveal the chemical dynamics, we are transforming the experimental data from the laboratory to the center-of-mass (CM) reference frame. First, fits of both the TOF spectra and the laboratory angular distribution could be achieved with a single channel for the reaction of silicon ( $^{28}$ Si; 28 amu) with thiomethanol (CH $_3$ <sup>32</sup>SH; 48 amu). This yields reaction products with a mass combination of 61 amu (H $^{28}$ Si $^{32}$ S) and 15 amu (CH $_3$ ). In detail, fits were accomplished with a center-of-mass translational energy distribution with a maximum translational energy ( $E_{max}$ ) of 83  $\pm$  9 kJ mol $^{-1}$ . Energy conservation dictates that for those reaction products formed without internal excitation, the high

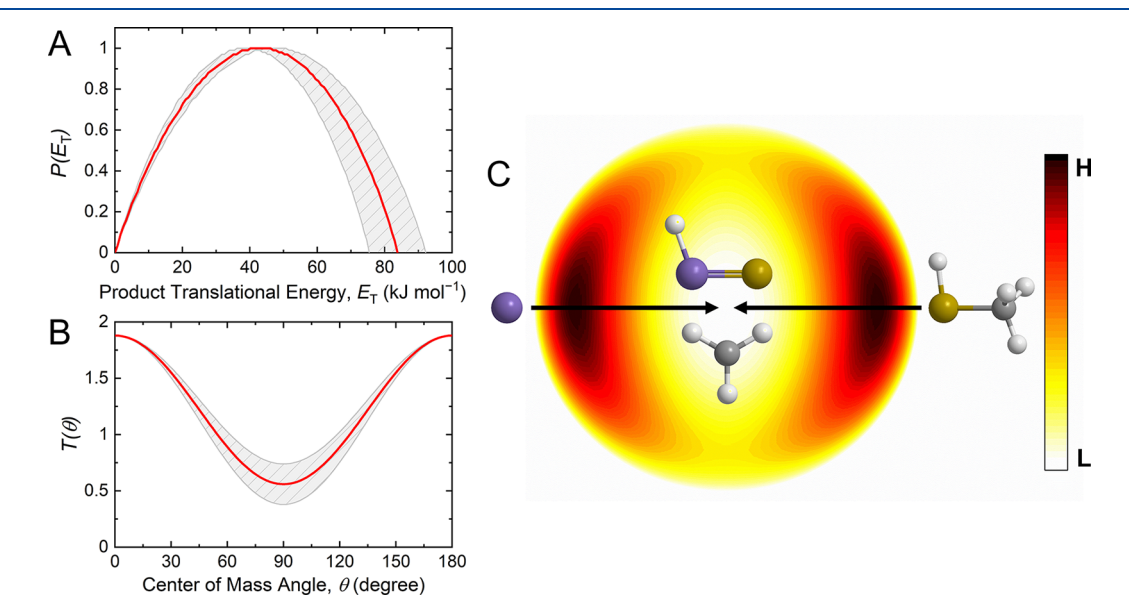


Figure 3. Center-of-mass product translational energy (A) and angular (B) flux distributions, as well as the corresponding flux contour map (C) of the reaction of atomic silicon ( $Si(^3P_j)$ ) with thiomethanol ( $CH_3SH$ ) leading to the formation of HSiS (m/z=61). Red lines define the best-fit functions while shaded areas denote the error limits. Atoms are colored as follows: silicon (purple); sulfur (yellow); carbon (gray); hydrogen (white).

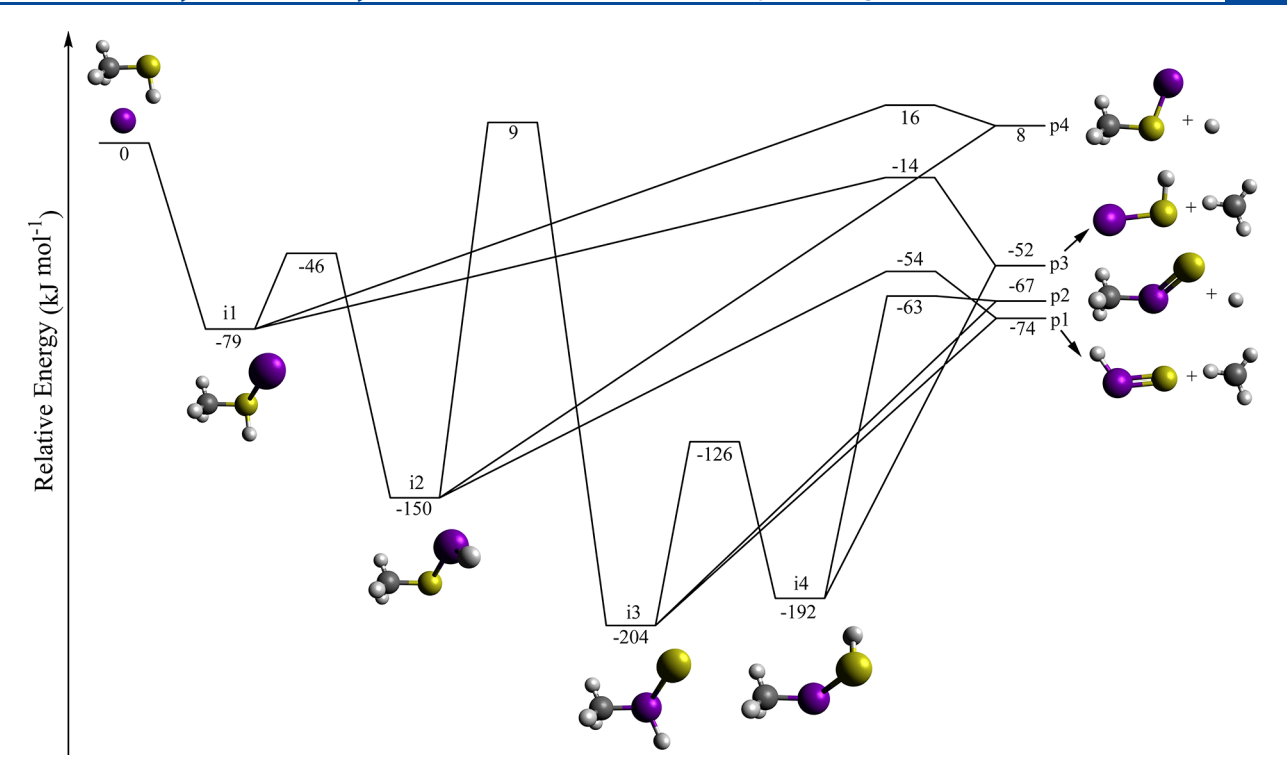


Figure 4. Schematic representation of the potential energy surface for the reaction between ground-state atomic silicon and thiomethanol calculated at the CCSD(T)-F12/aug-cc-pV(T+d)Z//M06-2X/cc-pV(T+d)Z+ZPE(M06-2X/cc-pV(T+d)Z) level of theory. The surface has been simplified by removing products above the reaction collision energy of 12.8 kJ mol<sup>-1</sup>; the full diagram is shown in Figure S3. Atoms are colored as follows: silicon (purple); sulfur (yellow); carbon (gray); hydrogen (white). Cartesian coordinates and vibrational frequencies are compiled in Table S2.

energy cutoff represents the sum of the reaction exoergicity plus the collision energy  $E_c$  (12.8  $\pm$  0.5 kJ mol<sup>-1</sup>). Therefore, by subtracting the collision energy from  $E_{\text{max}}$ , the methyl group loss channel is exoergic by  $70 \pm 10 \text{ kJ mol}^{-1}$ . Further, the  $P(E_{\rm T})$  peaks away from zero translational energy at about 43 kJ mol<sup>-1</sup>, suggesting a tight exit transition state of the decomposing reaction intermediate. This goes along with a substantial rearrangement of the electron density to form HSiS/HSSi plus the methyl radical. Finally, the  $T(\theta)$  is forward-backward symmetric and depicts intensity from 0° to 180°. These findings reveal indirect scattering dynamics through long-lived CH<sub>4</sub>SSi intermediate(s) with lifetimes longer than or at least comparable with their rotation periods. The distribution minimum at 90° proposes geometrical limitations and an emission of the methyl group nearly perpendicularly to the total angular momentum vector nearly within the rotational plane of the fragmenting complex(es).<sup>3</sup> These findings are also compiled in the flux contour maps (Figure 3).

What are the underlying reaction dynamics of the elementary reaction of atomic silicon with thiomethanol? First, we are contrasting the experimentally derived reaction energy of  $-70 \pm 10$  kJ mol<sup>-1</sup> with the theoretically predicted reaction energies to form the thiosilaformyl (HSiS,  $X^2A'$ ) and isothiosilaformyl (HSSi,  $X^2A'$ ) isomers of  $-74 \pm 5$  and  $-52 \pm 5$  kJ mol<sup>-1</sup> for reactions 3a and 3b, respectively. This comparison suggests that at least the thermodynamically more stable thiosilaformyl isomer (HSiS,  $X^2A'$ ) is formed; the preparation of the less stable isothiosilaformyl isomer (HSSi,  $X^2A'$ ) cannot be excluded at the present stage. Further, considering the molecular structures of the polyatomic reactant (CH<sub>3</sub>-S-H) and products (CH<sub>3</sub>, H-Si=S), it is evident that

the reacting silicon atom forms a bond with the sulfur atom and that the hydrogen atom is migrating from the sulfur atom to the silicon atom. Considering these experimental findings, we propose that ground-state atomic silicon interacts with one of the nonbonding electron pairs of the sulfur atom forming a sulfur-silicon bond via indirect (complex-forming) reaction dynamics. This leads to a CH<sub>3</sub>(H)SSi reaction intermediate which undergoes atomic hydrogen migration from the sulfur to the silicon atom yielding a CH<sub>3</sub>-S-Si-H intermediate. The latter could undergo unimolecular decomposition through the loss of a methyl group accompanied by formation of the thiosilaformyl isomer (HSiS, X2A') in an overall exoergic reaction  $(-70 \pm 10 \text{ kJ mol}^{-1})$ . The tight exit transition state can be rationalized through a significant electron reorganization from a sulfur-silicon single bond in the decomposing CH<sub>3</sub>-S-Si-H intermediate to a silicon-sulfur double bond in the thiosilaformyl radical product (HSiS,  $X^2A'$ ). It should be noted that intersystem crossing (ISC) from the triplet to the singlet surface might be relevant if "heavy" reactants such as silicon and/or sulfur are involved in elementary reactions. However, our experimental data alone neither support nor refute the involvement of nonadiabatic reaction dynamics, and the data presented here can be explained through reaction on the triplet surface only.

The experimental findings and reaction mechanisms proposed above are fully supported by the results from our electronic structure calculations (Figure 4). Ground-state atomic silicon adds barrierlessly to one of the two nonbonding electron pairs of the sulfur atom of hydrogen sulfide forming a weakly stabilized reaction intermediate i1 on the triplet surface. This intermediate can decompose via methyl loss by overcoming a barrier of 38 kJ mol<sup>-1</sup> with respect to the

separated products to p3 (HSSi; X<sup>2</sup>A') in an overall exoergic reaction by -52 kJ mol<sup>-1</sup>. Alternatively, i1 isomerizes via hydrogen shift from the sulfur to the silicon atom yielding i2; the barrier for the hydrogen shift is lower by 32 kJ mol<sup>-1</sup> compared to the exit barrier to form the methyl radical plus p3 (HSSi; X<sup>2</sup>A'). Note that atomic hydrogen losses from i1 and i2 to p4 (H<sub>3</sub>CSSi) are predicted to be endoergic by 8 kJ mol<sup>-1</sup>. Intermediate i2 can also undergo unimolecular decomposition via methyl loss to yield p1 (HSiS; X<sup>2</sup>A') after overcoming a tight transition state located 20 kJ mol<sup>-1</sup> above the separated products. Finally, our calculations also predict that a methyl group migration from i2 to i3 followed by hydrogen shift to i4 is likely unfavorable energetically upon comparing the energies of the transition state of  $i2 \rightarrow i3$  and of  $i2 \rightarrow p1 + CH_3$ , which favor the methyl loss exit channel by 63 kJ mol<sup>-1</sup>. The methyl group migration is accompanied by a significant elongation of the C-S bond from 183 to 217 pm; following this stretching mode of the methyl loss to p1 represents a much more favorable pathway. Therefore, although the atomic hydrogen loss channel to p2 (H<sub>3</sub>CSiS) is thermodynamically favorable compared to the formation of p1 (HSiS; X<sup>2</sup>A') plus methyl, the hydrogen loss pathway is closed considering the unfavorable barrier for the methyl migration  $(i2 \rightarrow i3)$ , which cannot compete compared to the unimolecular decomposition of i2 (i2  $\rightarrow$  p1 + CH<sub>3</sub>). This conclusion gains full support from our experimental findings and the lack of observation of the atomic hydrogen loss pathway (reaction 1) to form p2. The Rice-Ramsperger-Kassel-Marcus (RRKM) calculations also support these conclusions. Because the rate constants were evaluated with a collision energy of 0 kJ mol<sup>-1</sup> to simulate cold molecular cloud conditions, intermediates i3 and i4, as well as products p2 and p4, are inaccessible within the branching ratio calculations. This leaves products p1 and p3, which were predicted to be formed with a branching ratio of 98 to 2%, respectively. Consequently, it follows that the most prominent reaction pathway involves the addition of ground-state atomic silicon to the sulfur atom, hydrogen migration from i1 to i2 through a barrier 33 kJ mol<sup>-1</sup> above i1, and methyl loss through a tight exit transition state 20 kJ mol<sup>-1</sup> above the separated products ( $p1 + CH_3$ ). Note that the geometry of the exit transition state from i2 and p1 plus methyl depicts the methyl group ejected at angles of 74.9° and 89.7° with respect to the O-X and O-Y principal axes, respectively (Figure 5). This in-plane emission matches the

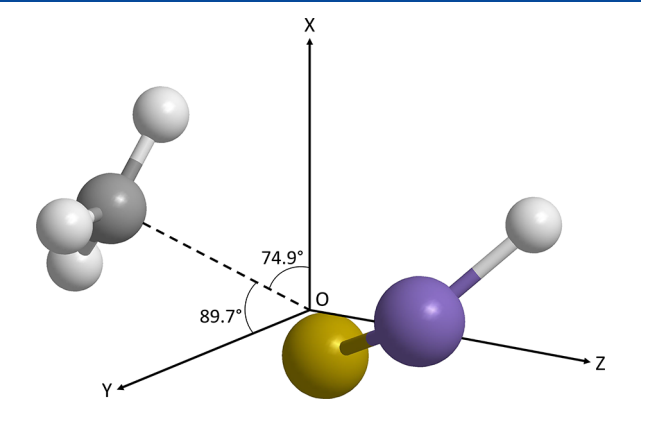


Figure 5. Orientation of the methyl leaving group in the transition state leading to the formation of product p1 from intermediate i2. The center of mass is located at the origin, O.

experimental prediction of the ejection direction of the methyl group based on the  $T(\theta)$  and flux contour map shown in Figure 3 very well. This calculated reaction energy of  $-74 \pm 5$  kJ mol<sup>-1</sup> is also in agreement with the experimentally derived reaction energy of  $-70 \pm 10$  kJ mol<sup>-1</sup> for the formation of the thiosilaformyl radical (HSiS) plus methyl.

The crossed molecular beam experiments of the elementary reaction of ground-state silicon atoms (Si(3Pi)) with thiomethanol (CH3SH) revealed the formation of at least the hitherto astronomically elusive thiosilaformyl isomer (HSiS, X<sup>2</sup>A') via indirect scattering dynamics. This isomer can be visualized as the "double heavy" substituted formyl radical (HCO, X<sup>2</sup>A'), which is known to exist in the interstellar medium since 1976.32 Likewise, the thiosilaformyl isomer (HSiS, X<sup>2</sup>A') can be connected to the recently observed thioformyl isomer (HCS, X<sup>2</sup>A')<sup>33</sup> by formally replacing the carbon atom through the isovalent silicon atom, hence providing the homologous series of isovalent <sup>2</sup>A' doublet radicals formyl, thioformyl, and thiosilaformyl: HCO, HCS, and HSiS. The H-E bond lengths of the formyl (HCO), thioformyl (HCS), and thiosilaformyl (HSiS) radicals of 1.120, 1.089, and 1.509 Å, respectively, as well as the E=Y doublebond lengths of 1.183, 1.568, and 1.967 Å, 34 indicate weaker and less energetic bonding involving silicon in comparison to carbon, especially with respect to the double bond between the heavy atoms.

With formyl (HCO) and thioformyl (HCS) observed toward, e.g., NGC 2024<sup>35</sup> and L483,<sup>33</sup> respectively, and the microwave spectrum of thiosilaformyl (HSiS) known from rotational spectroscopy studies, 36 the thiosilaformyl radical would represent an ideal target for prospective astronomical searches in, for example, the star-forming region SgrB2, where thiomethanol (CH<sub>3</sub>SH) has been observed; the atomic silicon reactant is the degradation product of silane (SiH<sub>4</sub>) by the internal vacuum ultraviolet photon field and energetic galactic cosmic rays.<sup>37</sup> The thiosilaformyl radical (HSiS) could act as a tracer to constrain the chemical and physical conditions of the hitherto poorly constrained silicon and sulfur chemistries and the formation of the very first silicon-sulfur bond in deep space. Here, the thiosilaformyl radical (HSiS) could eventually be photolyzed to silicon monosulfide (SiS) or react with atomic hydrogen to yield molecular hydrogen and silicon monosulfide (SiS), which has been predicted computationally to occur barrierlessly with rate constants of a few  $10^{-10}$  cm<sup>3</sup> s<sup>-1</sup>.38,39</sup> Note that models advocate that silicon monosulfide (SiS( $X^1\Sigma^+$ )) represents the critical molecular building block initiating the chain of reactions that lead ultimately to sulfide dust grains.  $^{28-30}$ 

# **EXPERIMENTAL METHODS**

The experiments were performed with a universal crossed molecular beam machine. The Briefly, a pulsed supersonic ground-state atomic silicon beam (Si( $^3P_j$ )) seeded in neon (Ne, 99.999%, Airgas) carrier gas was generated via laser ablation of a silicon rod kept in helical motion. Typically, 3 mJ of the 266 nm fourth harmonic output of a Nd:YAG laser are tightly focused onto a rotating silicon rod (Si, 99.999%, Goodfellow Cambridge Limited). The pulsed silicon atom beam with a velocity ( $\nu_p$ ) of 948  $\pm$  13 m s<sup>-1</sup> and speed ratio (S) of 6.0  $\pm$  0.3 crossed a pulsed thiomethanol (CH<sub>3</sub>SH, 98.0%, Sigma-Aldrich) beam ( $\nu_p$  = 740  $\pm$  18 m s<sup>-1</sup>, S = 10.2  $\pm$  0.8) kept at 550 Torr backing pressure perpendicularly in the interaction region of the scattering chamber. This resulted in a

collision energy of 12.8  $\pm$  0.5 kJ mol<sup>-1</sup> and center-of-mass angle of 54.0  $\pm$  1.1°. Reactively scattered species were monitored using a triply differentially pumped quadrupole mass spectrometer (QMS) with an electron-impact ionizer operated at 80 eV and 2 mA in 5° steps in the time-of-flight (TOF) mode. Up to 1.2  $\times$  10<sup>6</sup> TOF spectra were recorded at each angle. To gain information on the reaction dynamics, the TOF spectra and laboratory angular distribution were fit exploiting a forward convolution routine; this approach yielded the center-of-mass translational energy flux distribution  $P(E_{\rm T})$  along with the center-of-mass angular flux distribution  $T(\theta)$ . These functions were exploited to derive the flux contour map, denoted as  $I(u, \theta) \sim P(u) \times T(\theta)$ , which depicts an overall image of the outcome of the reaction.

# **■ COMPUTATIONAL METHODS**

The GAMESS-US<sup>42</sup> and MOLPRO<sup>43</sup> packages were employed in all calculations presented throughout this work. First, geometry optimizations and frequency analyses were performed at the density functional theory (DFT)<sup>44</sup> level employing the M06-2X<sup>45</sup> exchange and correlation functional, together with the cc-pV(T+d)Z basis set. 46,47 This functional was chosen for its performance in barrier heights (both hydrogen-transfer and non-hydrogen-transfer).<sup>48</sup> The calculations employed unrestricted wave functions; no symmetry restrictions were imposed. All transition states were confirmed to have a single imaginary frequency, and intrinsic reaction coordinate (IRC) calculations were performed for each of them to ensure the correct connection paths. To enhance the accuracy of the computed energies, we performed single-point energy calculations at the explicitly correlated coupled cluster <sup>49,50</sup> (CCSD(T)-F12) level, using the cc-pVTZ-F12 basis set <sup>51</sup> for all geometries previously optimized. The reported energies are always zero-point energy (ZPE) corrected at the DFT level, and the methodology is abbreviated as CCSD(T)-F12/aug-cc-pV(T+d)Z//M06-2X/ cc-pV(T+d)Z+ZPE(M06-2X/cc-pV(T+d)Z). This methodology usually yields energies with an accuracy of ±5 kJ mol<sup>-1</sup>. Energy-dependent rate constants (Table S1) were derived for the unimolecular reaction steps on the triplet CH<sub>4</sub>SiS PES following formation of the initial collision complex utilizing RRKM theory.<sup>52</sup> The available internal energy is the sum of the collision and chemical activation energies, where the value of the former used was 0 kJ mol<sup>-1</sup> to better simulate bimolecular reactions in cold molecular clouds. The rate constants were evaluated within the harmonic approximation with CCSD(T)-F12 energies and M06-2X/ccpV(T+d)Z vibrational frequencies. Statistical branching ratios between products were obtained from RRKM rate constants using the steady-state approximation.<sup>53</sup>

## ASSOCIATED CONTENT

# **Supporting Information**

The Supporting Information is available free of charge at https://pubs.acs.org/doi/10.1021/acs.jpclett.1c01706.

TOF spectra taken at the CM angle for m/z = 60 and 61 (Figure S1); Newton circle diagram for the title reaction (Figure S2); PES including all calculated products (Figure S3); energy-dependent rate constants derived from RRKM calculations (Table S1); computed Cartesian coordinates and vibrational frequencies of all

reactants, transition states, intermediates, and products (Table S2) (PDF)

## AUTHOR INFORMATION

#### **Corresponding Authors**

Breno R. L. Galvão — Centro Federal de Educação Tecnológica de Minas Gerais, CEFET-MG, 30421-169 Belo Horizonte, Minas Gerais, Brazil; o orcid.org/000-0002-4184-2437; Email: brenogalvao@gmail.com

Ralf I. Kaiser — Department of Chemistry, University of Hawai'i at Mānoa, Honolulu, Hawaii 96822, United States; orcid.org/0000-0002-7233-7206; Email: ralfk@hawaii.edu

#### **Authors**

Shane J. Goettl — Department of Chemistry, University of Hawai'i at Mānoa, Honolulu, Hawaii 96822, United States Zhenghai Yang — Department of Chemistry, University of Hawai'i at Mānoa, Honolulu, Hawaii 96822, United States Srinivas Doddipatla — Department of Chemistry, University of Hawai'i at Mānoa, Honolulu, Hawaii 96822, United States Chao He — Department of Chemistry, University of Hawai'i at Mānoa, Honolulu, Hawaii 96822, United States

Márcio O. Alves – Centro Federal de Educação Tecnológica de Minas Gerais, CEFET-MG, 30421-169 Belo Horizonte, Minas Gerais, Brazil

Complete contact information is available at: https://pubs.acs.org/10.1021/acs.jpclett.1c01706

#### Notes

The authors declare no competing financial interest.

## ACKNOWLEDGMENTS

The experimental studies were supported by the US National Science Foundation (NSF) under Award CHE-1853541. B.R.L.G. acknowledges financial support from Coordenação de Aperfeiçoamento de Pessoal de Nível Superior — Brasil (CAPES) - Finance Code 001 and Conselho Nacional de Desenvolvimento Científico e Tecnológico (CNPq, Grant 305469/2018-5).

## REFERENCES

- (1) Morfill, G. E.; Scholer, M. *Physical processes in interstellar clouds*; D. Reidel Publishing Company: Dordrecht, Holland, 1987.
- (2) Kaiser, R. I. Experimental investigation on the formation of carbon-bearing molecules in the interstellar medium via neutral-neutral reactions. *Chem. Rev.* **2002**, *102*, 1309.
- (3) Kaiser, R.; Yamada, M.; Osamura, Y. A crossed beam and ab initio investigation of the reaction of hydrogen sulfide,  $H_2S$  ( $X^1A_1$ ), with dicarbon molecules,  $C_2$  ( $X^1\Sigma_g^+$ ). *J. Phys. Chem. A* **2002**, *106*, 4825.
- (4) Linke, R. A.; Frerking, M. A.; Thaddeus, P. Interstellar methyl mercaptan. *Astrophys. J.* **1979**, 234, L139.
- (5) Lees, R. M.; Mohammadi, M. A. Millimetre wave spectrum of methyl mercaptan. Can. J. Phys. 1980, 58, 1640.
- (6) Turner, B. E. A molecular line survey of Sagittarius B2 and Orion-KL from 70 to 115 GHz. I. The observational data. *Astrophys. J., Suppl. Ser.* **1989**, *70*, 539.
- (7) Belloche, A.; Müller, H. S. P.; Menten, K. M.; Schilke, P.; Comito, C. Complex organic molecules in the interstellar medium: IRAM 30 m line survey of Sagittarius B2(N) and (M). Astron. Astrophys. 2013, 559, A47.
- (8) Müller, H. S. P.; Belloche, A.; Xu, L.-H.; Lees, R. M.; Garrod, R. T.; Walters, A.; van Wijngaarden, J.; Lewen, F.; Schlemmer, S.;

- Menten, K. M. Exploring molecular complexity with ALMA (EMoCA): Alkanethiols and alkanols in Sagittarius B2 (N2). Astron. Astrophys. 2016, 587, A92.
- (9) Knowles, D. J.; Wang, T.; Bowie, J. H. Radical formation of amino acid precursors in interstellar regions? Ser, Cys and Asp. *Org. Biomol. Chem.* **2010**, *8*, 4934.
- (10) Majumdar, L.; Gratier, P.; Vidal, T.; Wakelam, V.; Loison, J.-C.; Hickson, K. M.; Caux, E. Detection of CH<sub>3</sub>SH in protostar IRAS 16293–2422. *Mon. Not. R. Astron. Soc.* **2016**, 458, 1859.
- (11) Lee, C.-F.; Li, Z.-Y.; Ho, P. T.; Hirano, N.; Zhang, Q.; Shang, H. Formation and atmosphere of complex organic molecules of the HH 212 protostellar disk. *Astrophysical Journal* **2017**, 843, 27.
- (12) Vasyunin, A. I.; Herbst, E. Reactive desorption and radiative association as possible drivers of complex molecule formation in the cold interstellar medium. *Astrophys. J.* **2013**, 769, 34.
- (13) Lamberts, T. From interstellar carbon monosulfide to methyl mercaptan: Paths of least resistance. Astron. Astrophys. 2018, 615, L2.
- (14) Hiraoka, K.; Ohashi, N.; Kihara, Y.; Yamamoto, K.; Sato, T.; Yamashita, A. Formation of formaldehyde and methanol from the reactions of H atoms with solid CO at 10–20 K. *Chem. Phys. Lett.* **1994**, 229, 408.
- (15) Heays, A. N.; Bosman, A. D.; van Dishoeck, E. F. Photodissociation and photoionisation of atoms and molecules of astrophysical interest. *Astron. Astrophys.* **2017**, *602*, A105.
- (16) Williams, T. L.; Adams, N. G.; Babcock, L. M. Selected ion flow tube studies of  $H_3O^+(H_2O)_{0.1}$  reactions with sulfides and thiols. *Int. J. Mass Spectrom. Ion Processes* **1998**, *172*, 149.
- (17) Balucani, N.; Zhang, F.; Kaiser, R. I. Elementary reactions of boron atoms with hydrocarbons—Toward the formation of organoboron compounds. *Chem. Rev.* **2010**, *110*, 5107.
- (18) Kaiser, R. I.; Mebel, A. M. On the formation of polyacetylenes and cyanopolyacetylenes in Titan's atmosphere and their role in astrobiology. *Chem. Soc. Rev.* **2012**, *41*, 5490.
- (19) Parker, D. S. N.; Mebel, A. M.; Kaiser, R. I. The role of isovalency in the reactions of the cyano (CN), boron monoxide (BO), silicon nitride (SiN), and ethynyl ( $C_2H$ ) radicals with unsaturated hydrocarbons acetylene ( $C_2H_2$ ) and ethylene ( $C_2H_4$ ). Chem. Soc. Rev. 2014, 43, 2701.
- (20) Kaiser, R.; Sun, W.; Suits, A. Crossed beam reaction of atomic carbon  $C(^3P_j)$  with hydrogen sulfide,  $H_2S(X^1A_1)$ : Observation of the thioformyl radical, HCS  $(X^2A')$ . J. Chem. Phys. 1997, 106, 5288.
- (21) Ochsenfeld, C.; Kaiser, R. I.; Lee, Y. T.; Head-Gordon, M. Coupled-cluster ab initio investigation of singlet/triplet CH<sub>2</sub>S isomers and the reaction of atomic carbon with hydrogen sulfide to HCS/HSC. J. Chem. Phys. **1999**, 110, 9982.
- (22) Galland, N.; Caralp, F.; Rayez, M.-T.; Hannachi, Y.; Loison, J.-C.; Dorthe, G.; Bergeat, A. Reaction of carbon atoms, C (2p<sup>2</sup>, <sup>3</sup>P), with hydrogen sulfide, H<sub>2</sub>S (X<sup>1</sup>A<sub>1</sub>): Overall rate constant and product channels. *J. Phys. Chem. A* **2001**, *105*, 9893.
- (23) Doddipatla, S.; He, C.; Kaiser, R. I.; Luo, Y.; Sun, R.; Galimova, G. R.; Mebel, A. M.; Millar, T. J. A chemical dynamics study on the gas phase formation of thioformaldehyde (H<sub>2</sub>CS) and its thiohydroxycarbene isomer (HCSH). *Proc. Natl. Acad. Sci. U. S. A.* **2020**, *117*, 22712.
- (24) Dickinson, D. F.; Kuiper, E. N. R. Interstellar silicon sulfide. *Astrophys. J.* **1981**, 247, 112.
- (25) Schöier, F. L.; Bast, J.; Olofsson, H.; Lindqvist, M. The abundance of SiS in circumstellar envelopes around AGB stars. *Astron. Astrophys.* **2007**, *473*, 871.
- (26) Tercero, B.; Vincent, L.; Cernicharo, J.; Viti, S.; Marcelino, N. A line-confusion limited millimeter survey of Orion KL-II. Siliconbearing species. *Astron. Astrophys.* **2011**, *528*, A26.
- (27) Rosi, M.; Mancini, L.; Skouteris, D.; Ceccarelli, C.; Lago, N. F.; Podio, L.; Codella, C.; Lefloch, B.; Balucani, N. Possible scenarios for SiS formation in the interstellar medium: Electronic structure calculations of the potential energy surfaces for the reactions of the SiH radical with atomic sulphur and S<sub>2</sub>. Chem. Phys. Lett. **2018**, 695, 87.

- (28) Cherchneff, I. A chemical study of the inner winds of asymptotic giant branch stars. *Astron. Astrophys.* **2006**, *456*, 1001.
- (29) Smolders, K.; Neyskens, P.; Blommaert, J. A. D. L.; Hony, S.; Van Winckel, H.; Decin, L.; Van Eck, S.; Sloan, G. C.; Cami, J.; Uttenthaler, S.; et al. The Spitzer spectroscopic survey of S-type stars. *Astron. Astrophys.* **2012**, *540*, A72.
- (30) Massalkhi, S.; Agúndez, M.; Cernicharo, J. Study of CS, SiO, and SiS abundances in carbon star envelopes: Assessing their role as gas-phase precursors of dust. *Astron. Astrophys.* **2019**, *628*, A62.
- (31) Miller, W. B.; Safron, S. A.; Herschbach, D. R. Exchange reactions of alkali atoms with alkali halides: A collision complex mechanism. *Discuss. Faraday Soc.* 1967, 44, 108.
- (32) Snyder, L. E.; Hollis, J. M.; Ulich, B. L. Radio detection of the interstellar formyl radical. *Astrophys. J.* **1976**, 208, L91.
- (33) Agúndez, M.; Marcelino, N.; Cernicharo, J.; Tafalla, M. Detection of interstellar HCS and its metastable isomer HSC: New pieces in the puzzle of sulfur chemistry. *Astron. Astrophys.* **2018**, *611*, I.1
- (34) Woon, D. E.; Herbst, E. Quantum chemical predictions of the properties of known and postulated neutral interstellar molecules. *Astrophys. J., Suppl. Ser.* **2009**, *185*, 273.
- (35) Hollis, J. M.; Churchwell, E. Comparison of C<sup>+</sup> distributions with new interstellar sources of HCO emission. *Astrophys. J.* **1983**, 271, 170.
- (36) Brown, F. X.; Yamamoto, S.; Saito, S. The microwave spectrum of the HSiS radical in the <sup>2</sup>A' ground electronic state. *J. Mol. Struct.* **1997**, *413*, 537.
- (37) Suto, M.; Lee, L. C. Quantitative photoexcitation study of SiH<sub>4</sub> in vacuum ultraviolet. *J. Chem. Phys.* **1986**, *84*, 1160.
- (38) Paiva, M. A. M.; Lefloch, B.; Galvão, B. R. L. SiS formation via gas phase reactions between atomic silicon and sulphur-bearing species. *Mon. Not. R. Astron. Soc.* **2020**, 493, 299.
- (39) Doddipatla, S.; He, C.; Goettl, S.; Kaiser, R. I.; Galvão, B. R. L.; Millar, T. J. Non-adiabatic reaction dynamics to silicon monosulfide (SiS) A key molecular building block to sulfur-rich interstellar grains. *Sci. Adv.* **2021**, *7*, eabg7003 DOI: 10.1126/sciadv.abg7003.
- (40) Gu, X.; Guo, Y.; Kaiser, R. I. Mass spectrum of the butadiynyl radical ( $C_4H$ ;  $X^{2+}$ ). Int. J. Mass Spectrom. **2005**, 246, 29.
- (41) Gu, X.; Guo, Y.; Kawamura, E.; Kaiser, R. I. Characteristics and diagnostics of an ultrahigh vacuum compatible laser ablation source for crossed molecular beam experiments. *J. Vac. Sci. Technol., A* **2006**, 24, 505
- (42) Schmidt, M. W.; Baldridge, K. K.; Boatz, J. A.; Elbert, S. T.; Gordon, M. S.; Jensen, J. H.; Koseki, S.; Matsunaga, N.; Nguyen, K. A.; Su, S.; et al. General atomic and molecular electronic structure system. *J. Comput. Chem.* **1993**, *14*, 1347.
- (43) Werner, H. J.; Knowles, P. J.; Knizia, G.; Manby, F. R.; Schütz, M.; Celani, P.; Györffy, W.; Kats, D.; Korona, T.; Lindh, R. et al. *MOLPRO*, version 2015.1, a package of ab initio programs. 2015 http://www.molpro.net.
- (44) Kohn, W.; Sham, L. J. Self-consistent equations including exchange and correlation effects. *Phys. Rev.* **1965**, *140*, A1133.
- (45) Zhao, Y.; Truhlar, D. G. The M06 suite of density functionals for main group thermochemistry, thermochemical kinetics, noncovalent interactions, excited states, and transition elements: Two new functionals and systematic testing of four M06-class functionals and 12 other functionals. *Theor. Chem. Acc.* 2008, 120, 215.
- (46) Dunning Jr, T. H.; Peterson, K. A.; Wilson, A. K. Gaussian basis sets for use in correlated molecular calculations. X. The atoms aluminum through argon revisited. *J. Chem. Phys.* **2001**, *114*, 9244.
- (47) Kendall, R. A.; Dunning Jr, T. H.; Harrison, R. J. Electron affinities of the first-row atoms revisited. Systematic basis sets and wave functions. *J. Chem. Phys.* **1992**, *96*, 6796.
- (48) Peverati, R.; Truhlar, D. G. M11-L: A local density functional that provides improved accuracy for electronic structure calculations in chemistry and physics. *J. Phys. Chem. Lett.* **2012**, *3*, 117.
- (49) Adler, T. B.; Knizia, G.; Werner, H.-J. A simple and efficient CCSD (T)-F12 approximation. J. Chem. Phys. 2007, 127, 221106.

- (50) Knizia, G.; Adler, T. B.; Werner, H.-J. Simplified CCSD (T)-F12 methods: Theory and benchmarks. *J. Chem. Phys.* **2009**, *130*, 054104.
- (51) Peterson, K. A.; Adler, T. B.; Werner, H.-J. Systematically convergent basis sets for explicitly correlated wavefunctions: The atoms H, He, B-Ne, and Al-Ar. *J. Chem. Phys.* **2008**, *128*, 084102.
- (52) Eyring, H.; Lin, S. H. Basic chemical kinetics; John Wiley & Sons, Inc., 1980.
- (53) Kislov, V. V.; Nguyen, T. L.; Mebel, A. M.; Lin, S. H.; Smith, S. C. Photodissociation of benzene under collision-free conditions: An ab initio/Rice—Ramsperger—Kassel—Marcus study. *J. Chem. Phys.* **2004**, *120*, 7008.